Slurry transport of very large particles at high line speeds

Miedema, Sape

Publication date
2017

Document Version
Final published version

Published in
Proceedings 20th International Conference on Hydrotransport 2017

Citation (APA)
Miedema, S. (2017). Slurry transport of very large particles at high line speeds. In G. Coomes (Ed.), *Proceedings 20th International Conference on Hydrotransport 2017* (pp. 269-284). BHR Group Limited.

BHR Group
EXPERTS IN FLUID ENGINEERING

Slurry transport of very large particles at high line speeds

Sape A. Miedema
Delft University of Technology – Dredging Engineering

ABSTRACT

In slurry transport there are many models for fine, medium and coarse particles, based on the assumption that the particles are still small compared to the pipe diameter. However, when the particle size is not small compared to the pipe diameter (up to 25% of the pipe diameter) the models do not give a good prediction of the hydraulic gradient. The existing models assume suspended flow at high line speeds, but the question is, will there still be suspension in this case. Yagi, Vlasak, Ravelet and others carried out experiments with very large particles and describe the phenomena occurring, but do not give a physical or mathematical model for this case. At low line speeds the physics of the slurry transport can be described with the 2LM or 3LM models (Wilson, Doron, etc.), but at high line speeds these models are not sufficient. Will there be (pseudo) homogeneous transport at high line speeds or will there still be a sort of sliding bed (sliding flow)? How does the sliding friction coefficient behave? How does the slip velocity behave? Is there still a Limit Deposit Velocity?
To answer these questions the available experimental data from literature is investigated.
This paper shows a collection of experimental data from literature of different authors, shows the general trends and a model for very coarse particles at high line speeds.

1 INTRODUCTION

Vlasak et al. (2012) and (2014) investigated the transport of coarse particles in a **D_p=0.1 m** pipe in the Institute of Hydrodynamics in Prague. The particles had a **d_{50}=11.0-11.7 mm** diameter (so the particles had a diameter of about 10-11% of the pipe diameter) and were transported with line speeds in the range of 1.5 m/s to 5.5 m/s. The density of the particles is 2.787 ton/m^3 and the carrier liquid was water. Volumetric concentrations in the range of 3% to 15% were used.

In the horizontal pipe section the flow was significantly stratified. For low line speeds the individual particles were sliding and rolling over the bottom of the pipe. Increasing the line speed resulted in ripples and dunes. In the lower line speed range the sliding bed layer was combined with saltation on top of the bed and dunes appearing and disappearing. With increasing line speed the thickness of the sliding bed decreased and particle saltation became the dominant mode of particle movement. However, most particles remained in contact with the pipe wall. The pressure drops were mainly produced by mechanical friction between the particles and the pipe wall, also resulting in relatively high slip ratio

values. The transport was dominated by particle-particle interactions and particle-wall interactions. The horizontal particle velocities increased with the vertical distance from the pipe bottom. Saltating (free) particles had a much higher horizontal velocity compared with the particles in the bed.

The concentration distribution is important to understand the internal structure of the mixture flow. The higher concentrations shown at the top of the pipe were detected as errors due to the effect of the pipe material on gamma-ray absorption.

At low line speeds (Figure 1) the local concentration tends to approach zero at the upper portion of the pipe. This region increased with decreasing concentration and occupied 30%-50% of the pipe. A nearly linear concentration profile was observed in the lower part of the pipe, increasing from a bottom concentration at the bottom of the pipe to almost zero at a height of 50%-70% of the pipe. The bottom concentration decreased with a decreasing cross sectional averaged concentration. Very dense sand or gravel has a concentration up to 66%. Very loose sand or gravel a concentration of about 50%. Below a concentration of 50% the particles do not rest on top of each other, however in a fast-flowing sliding bed this is possible because of the kinetic particle-particle interactions.

Moderate line speeds (Figure 2) showed the same behavior, but with smaller bottom concentrations. At high line speeds (Figure 3) the bottom concentrations decreased further, but with the same shape of the concentration profile. In general, the particles tend to occupy the bottom part of the pipe and the concentration profile is symmetrical to the vertical plane of symmetry.

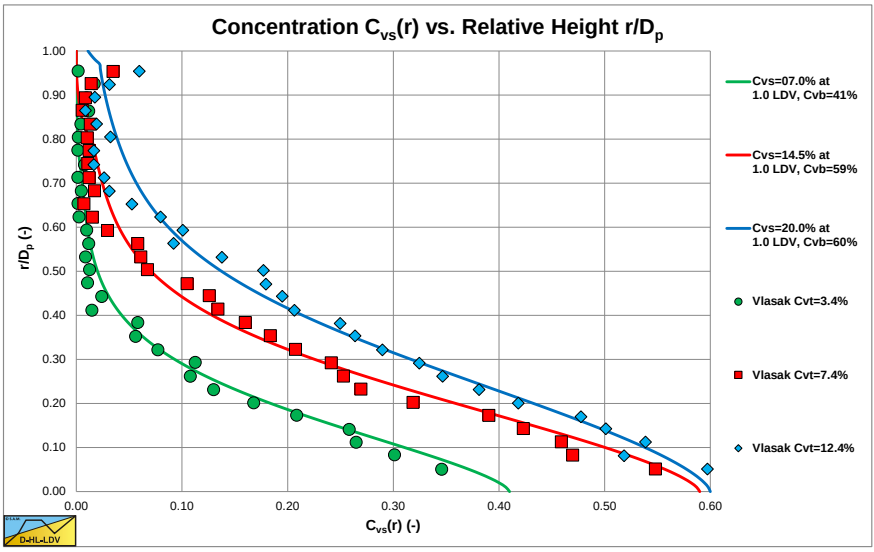

Figure 1: Experiments of Vlasak et al. (2014) in a D_p=0.1 m pipe and d=11 mm particles at v_{ls}=1.8 m/s.

According to the Delft Head Loss & Limit Deposit Velocity (DHLLDV) Framework of Miedema (June 2016) the maximum Limit Deposit Velocity (LDV) of the particles used by Vlasak et al. (2012) and (2014) has a value around 3 m/s (depending on the concentration). For small particles, this LDV is the velocity above which no stationary or sliding bed exists. It is the question however whether for large particles an LDV still exists

since the particles continue to occupy the bottom part of the pipe even at high line speeds. Maybe at low concentrations this may be the case, but at high concentrations there is not enough turbulent energy to completely remove the bed. It seems also at high line speeds there is still a sort of bed, but with decreased concentration as the line speed increases.

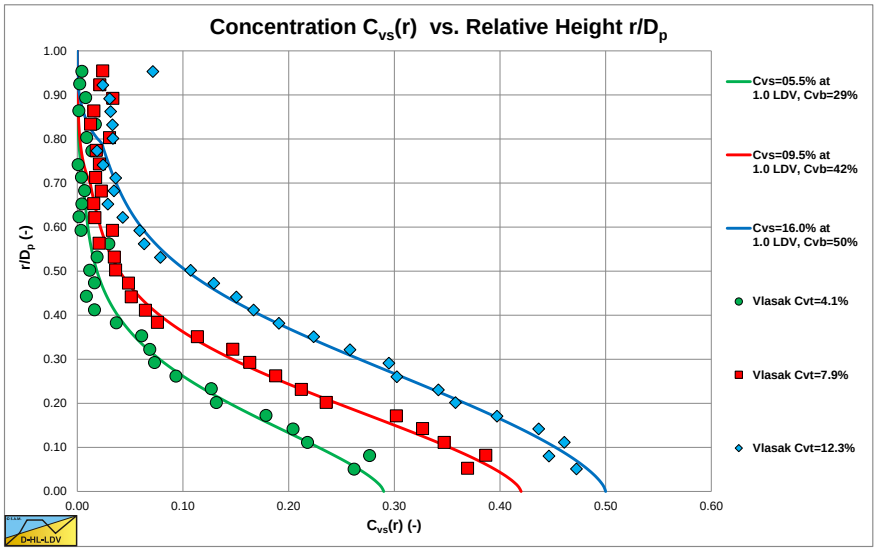

Figure 2: Experiments of Vlasak et al. (2014) in a D_p=0.1 m pipe and d=11 mm particles at v_{ls}=2.8 m/s.

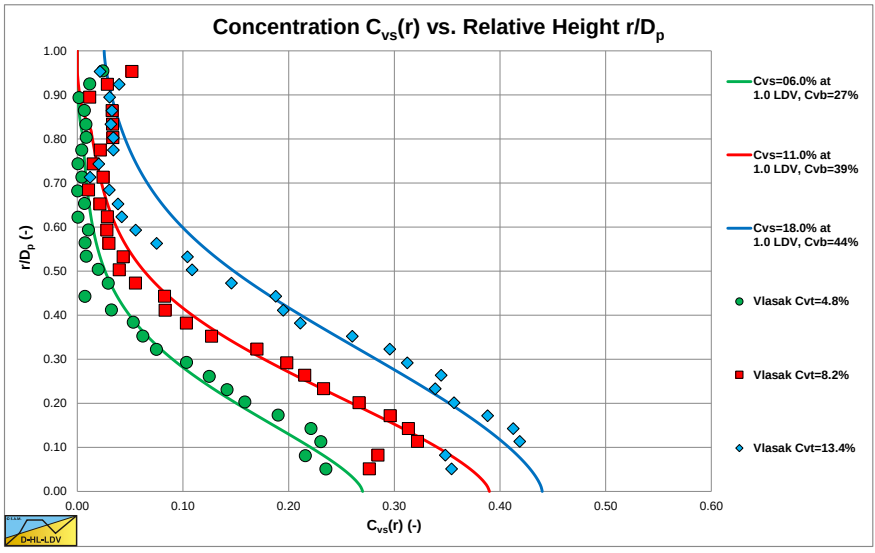

Figure 3: Experiments of Vlasak et al. (2014) in a D_p=0.1 m pipe and d=11 mm particles at v_{ls}=4.1 m/s.

Apparently very coarse particles do not follow the heterogeneous (based on potential and kinetic energy losses) and homogeneous (based on a particle free viscous sub-layer) flow

regimes at high line speeds as has been described by Miedema (June 2016), but follow a different behavior, which is named the sliding flow regime. In the sliding flow regime, the hydraulic gradient is dominated by sliding and/or rolling friction instead of collisions as in the heterogeneous regime. As long as the bed has a high concentration preventing the particles to start rolling, the normal sliding friction coefficient as used in the sliding bed regime can be applied. However, if the bed concentration reduces below 50%, giving particles more freedom to roll, the observed sliding friction coefficient may reduce because the rolling friction coefficient is always smaller than the sliding friction coefficient.

2 THE SLIDING FLOW REGIME

For fine and medium sized particles, there is a transition from a sliding bed to heterogeneous transport at a certain line speed. However, for large particles the turbulence is not capable of lifting the particles enough, resulting in a sort of sliding bed behavior above this transition line speed. One reason for this is that the largest eddies are not large enough with respect to the size of the particles.

Sellgren & Wilson (2007) use the criterion $\mathbf{d/D_p>0.015}$ for this to occur. They named this fully stratified flow. Probably the criterion is more complicated, based on a Reynolds or Froude number. This is subject to further research.

Zandi & Govatos (1967) use a factor $\mathbf{N<40}$ as a criterion, with (Froude number related):

$$\mathbf{N = \frac{v_{ls}^2 \cdot \sqrt{C_D}}{g \cdot R_{sd} \cdot D_p \cdot C_{vt}}} \qquad \mathbf{(1)}$$

This criterion is based on the line speed, the particle drag coefficient, the relative submerged density, the pipe diameter and the transport concentration. At the Limit Deposit Velocity $\mathbf{v_{ls,ldv}}$ this equation can be simplified for coarse particles by using the limiting factor of Durand & Condolios (1952) for the LDV Froude number and the particle Froude number (Gibert (1960)):

$$\mathbf{F_L = \frac{v_{ls,ldv}}{\sqrt{2 \cdot g \cdot D_p \cdot R_{sd}}} \approx 1.34 \quad and \quad \sqrt{C_D} \approx 0.6 \text{ for coarse particles}} \qquad \mathbf{(2)}$$

Giving:

$$\mathbf{N = \frac{v_{ls,ldv}^2 \cdot \sqrt{C_D}}{g \cdot R_{sd} \cdot D_p \cdot C_{vt}} = \left(\frac{v_{ls,ldv}^2}{2 \cdot g \cdot R_{sd} \cdot D_p} \right) \cdot \frac{2 \cdot \sqrt{C_D}}{C_{vt}}} \qquad \mathbf{(3)}$$

$$\mathbf{= 1.34^2 \cdot \frac{2 \cdot 0.6}{C_{vt}} = \frac{2.37}{C_{vt}}}$$

This gives $\mathbf{N=2.37/C_{vt}<40}$ or $\mathbf{C_{vt}>0.059}$ for sliding flow to occur. This criterion apparently is based on the thickness of sheet flow. If the bed is so thin that the whole bed becomes sheet flow, there will not be sliding flow, but more heterogeneous behavior. The values

used in both criteria are a first estimate based on literature and may be changed in the future. At higher line speeds this percentage decreases with the line speed squared, which seems reasonable.

Figure 4 shows experiments of Durand & Condolios (1952), showing heterogeneous and homogeneous behaviour of very small particles, heterogeneous behaviour of medium sized particles and sliding flow behaviour of large particles.

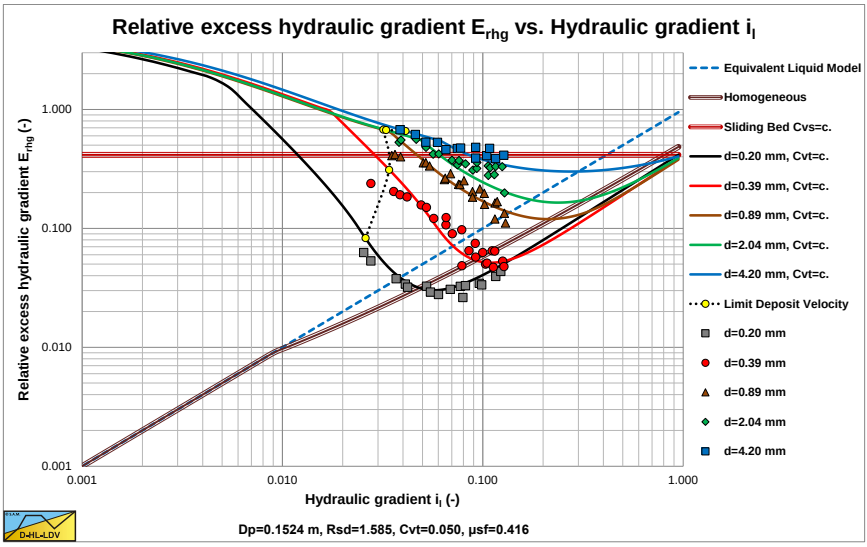

Figure 4: Experiments of Durand & Condolios (1952).

A pragmatic approach to determine the relative excess hydraulic gradient in the sliding flow regime is to use a weighted average between the heterogeneous regime and the sliding bed regime. Pragmatic because particles with $\mathbf{d=0.015 \cdot D_p}$ still show heterogeneous behavior, while much larger particles show sliding bed behavior. This approach gives a smooth transition.

First the factor between particle size and pipe diameter according to Sellgren & Wilson (2007) is determined:

$$\mathbf{f = \frac{d}{0.015 \cdot D_p}} \qquad \mathbf{(4)}$$

The factor of 0.015 is an estimate. Sellgren & Wilson (2007) give a range of 0.015-0.018, but this probably also depends on the solids density, the particle shape and the fluid properties.

Secondly the weighted average hydraulic gradient or relative excess hydraulic gradient is determined, based on the values in the heterogeneous regime and the sliding bed regime:

$$\mathbf{i_{m,SF} = \frac{i_{m,HeHo} + \left(f-1\right) \cdot i_{m,SB}\right)}{f} \text{ or } E_{rhg,SF} = \frac{E_{rhg,HeHo} + \left(f-1\right) \cdot \mu_{sf}}{f}} \qquad \mathbf{(5)}$$

Figure 5 and Figure 6 show the relative excess hydraulic gradient of nine particle diameters for a constant delivered volumetric concentration of 17.5% according to the DHLLDV Framework of Miedema (June 2016) and validated with experiments. The graphs also show the horizontal sliding bed curve for constant spatial volumetric concentration, the ELM curve and the homogeneous curve as a reference system. The LDV points for each particle diameter are also shown.

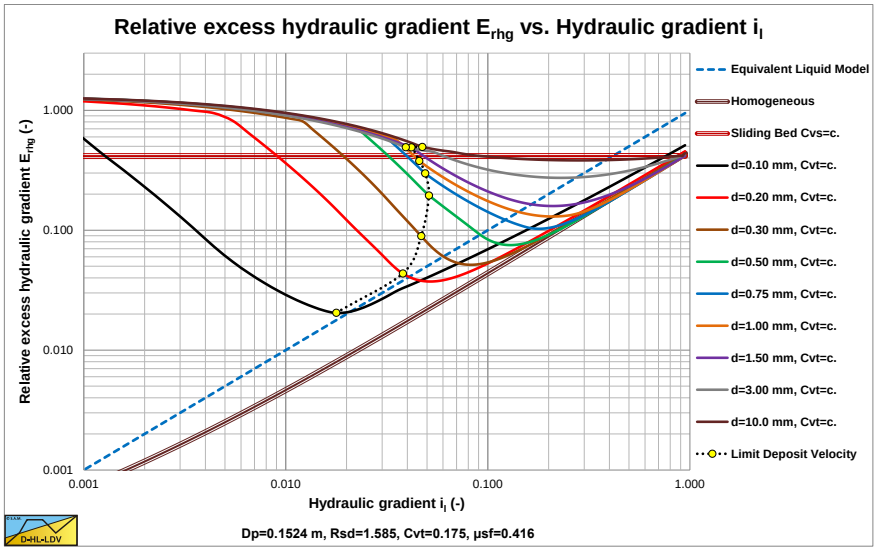

Figure 5: The relative excess hydraulic gradient as a function of the hydraulic gradient, constant C_{vt} and D_p=0.1524 m.

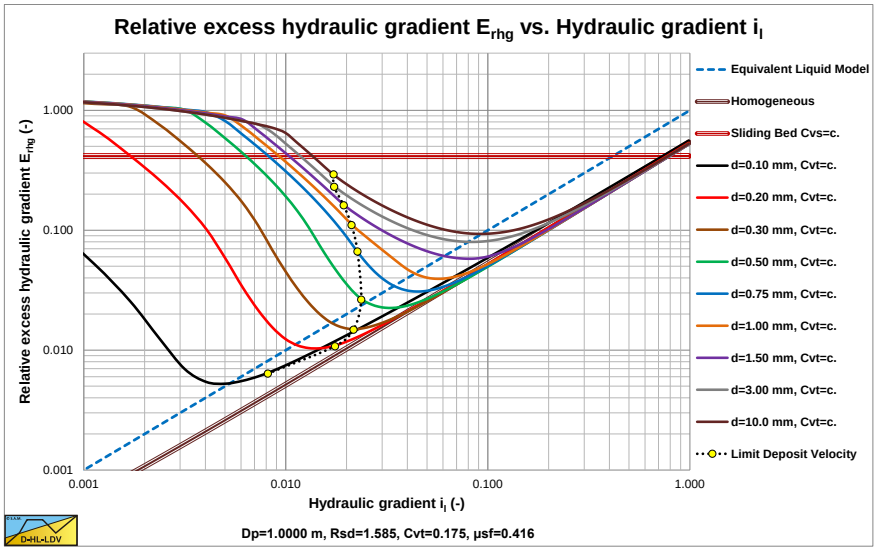

Figure 6: The relative excess hydraulic gradient as a function of the hydraulic gradient, constant C_{vt} and D_p=1 m.

Figure 5 shows that large particles in a **D_p=0.1524 m** pipe have a much less steep curve due to sliding flow than the smaller particles. Sliding flow starts with particles of about **d=2.3 mm** with this pipe diameter.

Figure 6 shows that this does not occur in a large **D_p=1 m** pipe. Here sliding flow starts with particles of about **d=15 mm**, which are not in the graph.

Apparently in a larger pipe the turbulent eddies are strong enough to bring larger particles in suspension. One should consider that the size of the largest eddies is proportional to the pipe diameter and the operational line speed increases with the pipe diameter to a power of about 0.4. So the operational Reynolds number will increase with the pipe diameter to a power of about 1.4. For the two examples given here this gives a factor of about 14 for the Reynolds number. The ratio of the largest to the smallest eddies, dissipating the turbulent energy into heat, equals the Reynolds number to a power of 0.75. This means that the smallest eddies have about similar size in both pipes under operational conditions.

It is interesting to compare the above method with existing models. Over the years the Wilson et al. (1992) sliding bed model and the Saskatchewan Research Council (SRC) (1993) model were calibrated with numerous experiments with a broad range of particle sizes, different particle densities and pipe diameters. Over the years both models have many modifications and additions. The latest versions are used here.

Although the author does not agree with all of the physics behind these models, the author feels these models give trustworthy results, based on the validation with numerous experiments. The author disagrees with the hydrostatic normal stress approach of the Wilson et al. (1992) model and the buoyancy effect of smaller fraction on larger fractions of the SRC model.

The Wilson et al. (1992) model, although based on constant spatial volumetric concentrations, only gives equations for constant delivered volumetric concentrations. These equations are achieved by interpolating constant spatial volumetric concentration curves, combined with the slip ratios determined. The SRC curves are determined for constant spatial volumetric concentrations. The DHLLDV Framework shows both curves, but the basis is constant spatial volumetric curves. Similar to Wilson et al. (1992), the delivered concentration curves are based on the slip ratio curve determined.

The resulting DHLLDV Framework curves match very well with the SRC model in the range of operational line speeds. Figure 7 and Figure 8 show this for a **d=3 mm** particle in a **D_p=0.1524 m** (6 inch) pipe. The SRC model used here is described in Miedema (June 2016) chapter 6, based on the weight approach for the sliding friction instead of the hydrostatic normal stress approach. The difference of the two approaches at operational line speeds is very small. The relative hydraulic excess gradient seems to differ, but in the hydraulic gradient graph it is clear that there is not much difference in the range of line speeds of 4 to 6 m/sec. Both the SRC model and the DHLLDV Framework are based on constant spatial volumetric concentration. The Wilson model gives a higher curve, but the Wilson model is based on a constant delivered volumetric concentration and the proportionality factor in this model has changed over time.

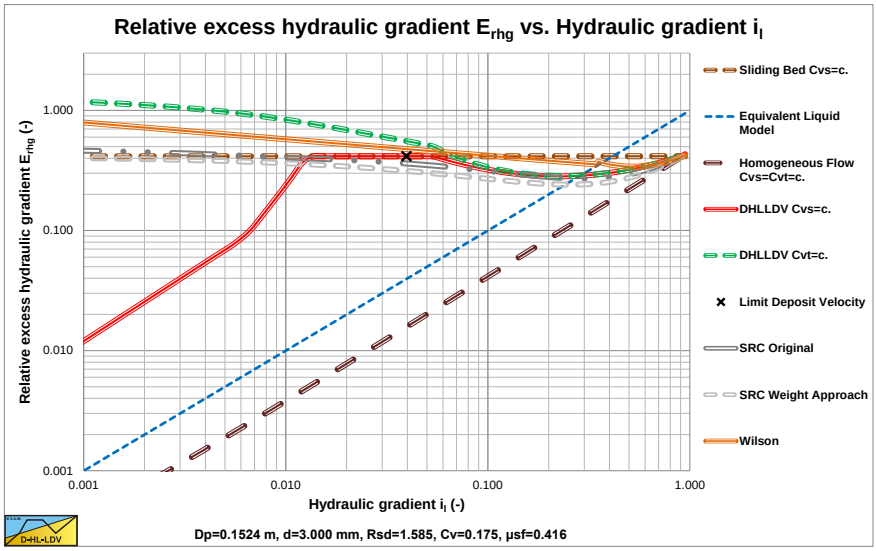

Figure 7: The sliding flow regime in the E_{rhg} vs. i_l graph.

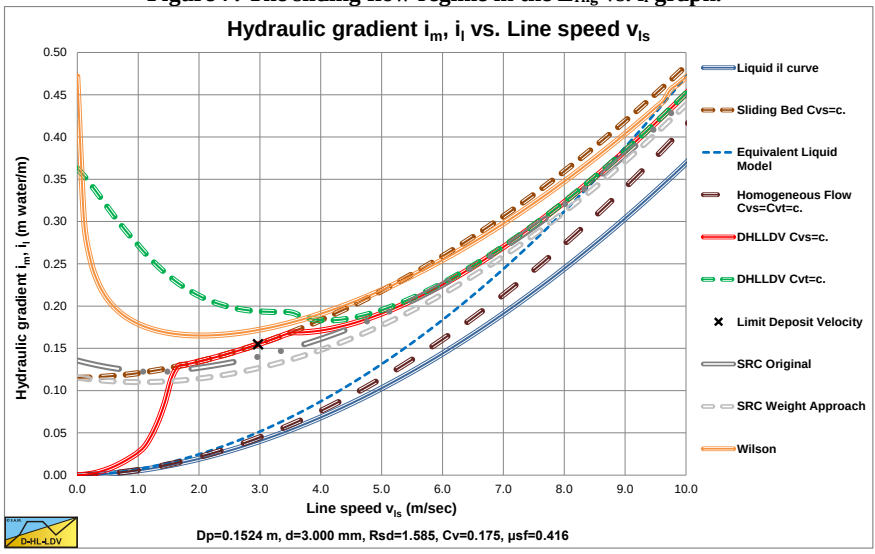

Figure 8: The sliding flow regime in the i_m vs. v_{ls} graph.

3 CONSTANT SPATIAL VOLUMETRIC CONCENTRATION

Figure 9 and Figure 10 show sliding flow behavior of experiments of Boothroyde et al. (1979) and Wiedenroth (1967) with constant spatial volumetric concentrations. The descending dash-dot-dot line shows heterogeneous behavior.

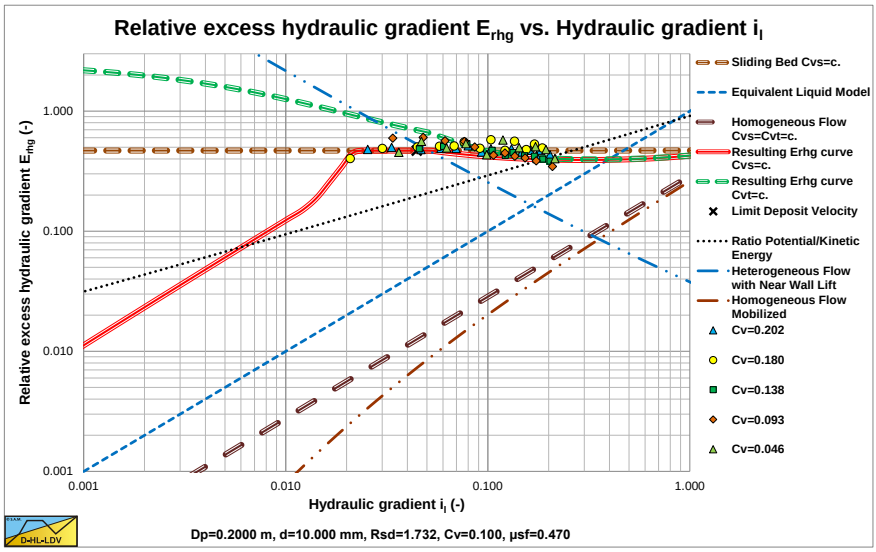

Figure 9: An example of sliding flow behavior, Boothroyde et al. (1979).

It is clear that the data points do not follow the descending heterogeneous curve, but continue almost horizontal following sliding flow behavior. Whether the relative excess hydraulic gradient decreases slightly at increasing line speeds (the hydraulic gradient) is difficult to observe due to the scatter.

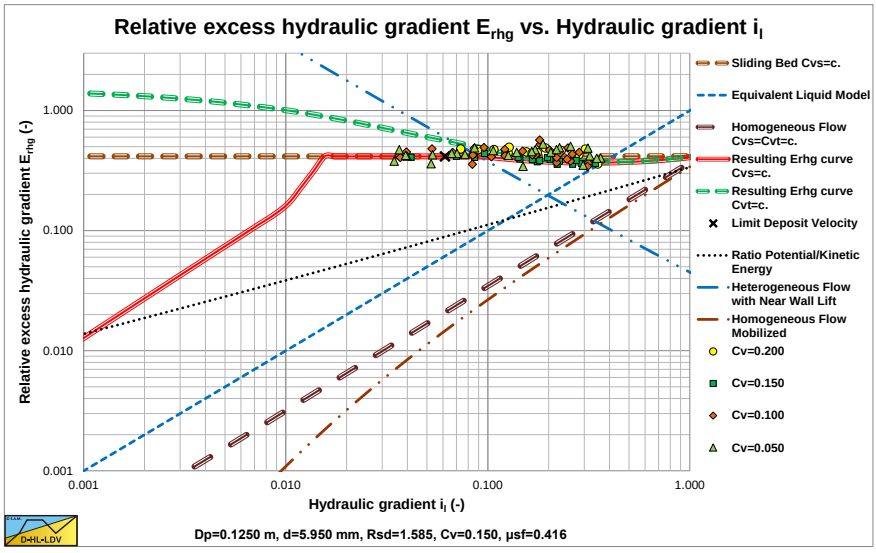

Figure 10: Another example of sliding flow behavior, Wiedenroth (1967).

4 CONSTANT DELIVERED VOLUMETRIC CONCENTRATION

Figure 11 and Figure 12 show constant delivered volumetric concentration curves of Doron & Barnea (1993). Figure 11 shows that at small concentrations the heterogeneous behavior is followed. Figure 12 shows that at larger concentrations this is not the case and sliding flow behavior is followed. It is interesting that Doron & Barnea (1993) used particles with a very small relative submerged density, still showing sliding flow behavior. Apparently, the particle diameter to pipe diameter ratio dominates this behavior and the relative submerged density is less important.

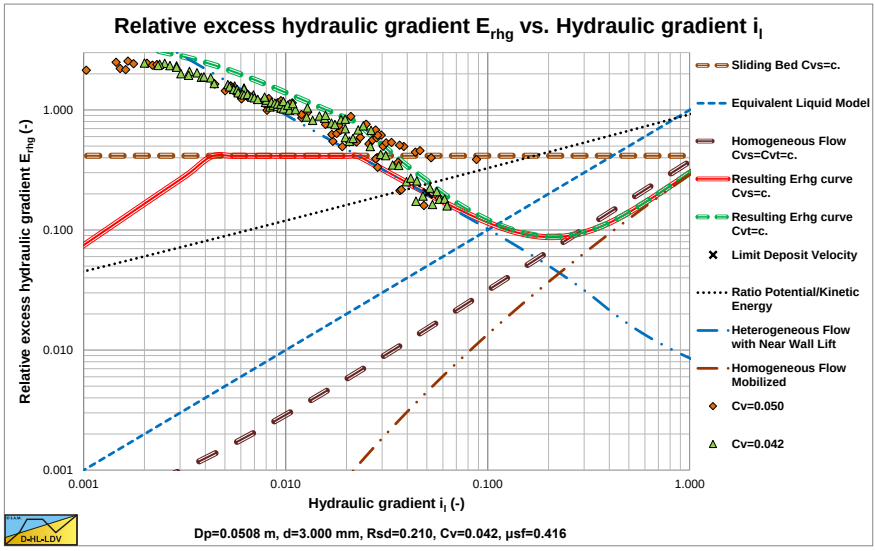

Figure 11: Heterogeneous behavior at low concentrations, Doron & Barnea (1993).

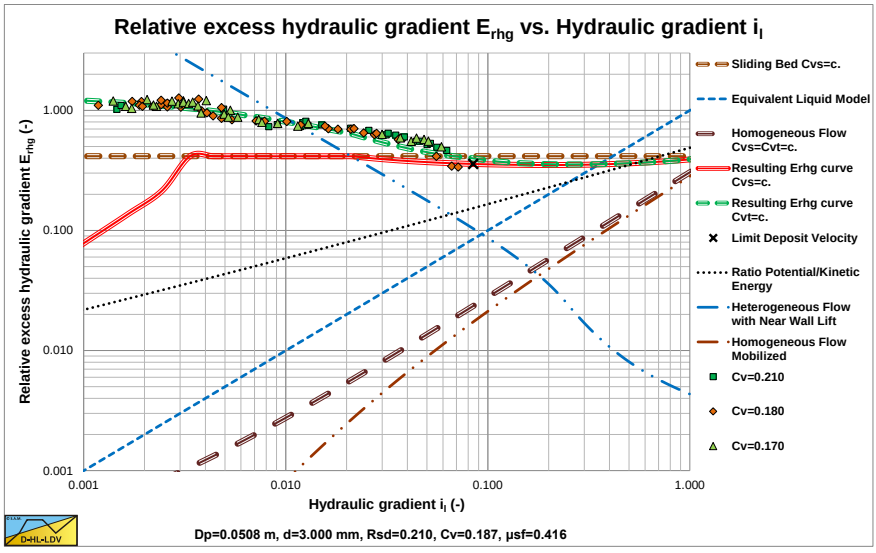

Figure 12: Sliding flow behavior at higher concentrations, Doron & Barnea (1993).

5 THE CONCENTRATION DISTRIBUTION.

The concentration in the pipe can be described according to Miedema (June 2016):

$$C_{vs}(r) = C_{vB} \cdot e^{-\frac{\alpha_{sm}}{C_{vr}} \cdot \left(\frac{v_{ls,ldv}}{v_{ls}} \right)^{0.925} \cdot \frac{v_{thv}}{v_{thv,ldv}} \cdot \frac{r}{D_p}} \qquad (6)$$

The bottom concentration is now for line speeds above the LDV:

$$C_{vB} = C_{vb} \cdot \left(\frac{v_{ls,ldv}}{v_{ls}} \right)^{0.925} \cdot \frac{v_{thv}}{v_{thv,ldv}} \qquad (7)$$

Now assuming that the terminal (hindered) settling velocity in the suspension hardly depends on the line speed, these equations can be written as:

The concentration in the pipe, without correction for the circular shape, can be described according to:

$$C_{vs}(r) = C_{vB} \cdot e^{-\frac{\alpha_{sm}}{C_{vr}} \cdot \left(\frac{v_{ls,ldv}}{v_{ls}} \right)^{0.925} \cdot \frac{r}{D_p}} \qquad (8)$$

The bottom concentration is now for line speeds above the LDV:

$$C_{vB} = C_{vb} \cdot \frac{\left(\alpha_{sm} \cdot \left(\frac{v_{ls,ldv}}{v_{ls}} \right)^{0.925} \right)}{\left(1 - e^{-\frac{\alpha_{sm}}{C_{vr}} \cdot \left(\frac{v_{ls,ldv}}{v_{ls}} \right)^{0.925}} \right)} \qquad (9)$$

These equations describe the concentration distribution well for 2D channel flow above the LDV. However, for a circular pipe and below the LDV some adjustments should be made. When the concentration found is integrated over the circular cross section of the pipe, the cross sectional averaged concentration should be equal to the average concentration that is input to the calculations, which might be the case for a symmetrical concentration distribution, but certainly not for an asymmetrical concentration distribution.

Now in the case of a circular pipe the vertical coordinate $\mathbf{r/D_p}$ should be replaced by the fraction of the cross-section **f**. This gives a much better match with the cross sectional averaged concentration in case there is no bed, so above the LDV. This fraction can be determined by the angle **β** matching a certain vertical coordinate, similar to the angle **β** for the stationary and sliding bed.

$$\beta = a\cos\left(\frac{0.5 - \frac{r}{D_p}}{0.5}\right) \quad (10)$$

The fraction **f** is now:

$$f = \frac{\beta - \sin(\beta)\cdot\cos(\beta)}{\pi} \quad (11)$$

The concentration at r/D_p is now:

$$C_{vs}(r) = C_{vB}\cdot e^{-\frac{\alpha_{sm}}{C_{vr}}\cdot\left(\frac{v_{ls,ldv}}{v_{ls}}\right)^{0.925}\cdot f} \quad (12)$$

The correction factor has to be determined at the LDV, giving an implicit equation with only the relative volumetric concentration as the parameter:

$$\alpha_{sm} = \left(1 - e^{-\frac{\alpha_{sm}}{C_{vr}}}\right) \quad (13)$$

The correction factor appears to depend only on the relative concentration C_{vr} according to:

$$\alpha_{sm} = 0.9847 + 0.304\cdot C_{vr} - 1.196\cdot C_{vr}^2 - 0.5564\cdot C_{vr}^3 + 0.47\cdot C_{vr}^4 \quad (14)$$

At low relative concentrations, $C_{vr}<0.3$, this factor is about 1. For sliding flow the LDV does not exist for determining the concentration distribution. The behavior is such that at each line speed it seems there is an LDV. So, the line speed can be removed from the concentration distribution equation, giving:

$$C_{vs}(r) = C_{vB}\cdot e^{-\frac{\alpha_{sm}}{C_{vr}}\cdot f} \quad (15)$$

In the case of **Sliding Flow**, the bottom concentration decreases with increasing line speed and with decreasing spatial concentration. Above a spatial concentration of 17.5% the bottom concentration decreases with increasing concentration. The bottom concentration can be determined with the following equation, where the bottom concentration can never be larger than the maximum bed concentration C_{vb}.

$$C_{vB} = 11.1\cdot C_{vb}\cdot\left(\frac{v_{ls,ldv}}{v_{ls}}\right)\cdot\left(C_{vs}\cdot\left(1 - \frac{C_{vs}}{0.175\cdot(1+\beta)}\right)^{\beta}\right) \quad (16)$$

The LDV in this equation is the LDV determined with Miedema (June 2016).

To determine the concentration distribution, the procedure outlined here should be followed with a line speed to Limit Deposit Velocity ratio of 1 and a bottom/bed concentration as determined with the above equation. Physically this means that a sliding bed will transit to sliding flow by increasing the porosity between the particles with increasing line speed.

Figure 1, Figure 2 and Figure 3 show experimental results of Vlasak et al. (2014) in a $\mathbf{D_p=0.1\ m}$ pipe and **d=11 mm** particles at 3 different line speeds. The $\mathbf{d/D_p}$ ratio equals 0.11, so this is certainly in the **Sliding Flow** regime. The experiments show a decreasing bottom concentration with increasing line speed and a decreasing bottom concentration with decreasing spatial concentration according to the above equation. The volumetric concentrations used to simulate the measured concentration profiles are higher than the volumetric concentrations mentioned by Vlasak et al. (2014). Most probably Vlasak et al. (2014) measured delivered concentrations, while here spatial concentrations have to be used. It should be mentioned that the experiments show some small concentration at the top of the pipe, which is a measurement error. The predictions and the experimental data however match well. These experimental concentration profiles required a factor 2 in the hindered settling power instead of the default value of 4.

6 VERIFICATION & VALIDATION

Figure 9 and Figure 10 show sliding flow behavior for two types of gravel, with **d=6 mm** and **d=10 mm** and constant spatial volumetric concentrations. At higher line speeds or liquid hydraulic gradients, the relative excess hydraulic gradient of the DHLLDV Framework tends to decrease slightly. This occurs when the liquid hydraulic gradient is close to the intersection point between the sliding bed/sliding flow curve and the ELM curve. In this region, however the line speeds are so high that there are hardly any experimental data available. The data here are obtained from Boothroyde et al. (1979) and Wiedenroth (1967).

Figure 11 and Figure 12 show heterogeneous behavior at very low concentrations and sliding flow behavior at higher concentrations. These experiments by Doron & Barnea (1993) were carried out with delivered volumetric concentration measurements. They clearly show that at very low concentrations there is still heterogeneous behavior, while the higher concentrations show sliding flow behavior.

The weighted average approach seems to give good results. Still the criterion for sliding flow, $\mathbf{d>0.015\cdot D_p}$, is too simple and requires more research.

For the concentration distribution, the bottom/bed concentration has to be determined first. Secondly the concentration profile can be determined based on a line speed to Limit Deposit Velocity ratio of 1.

In the sliding flow regime, the LDV doesn't really have a physical meaning. At high line speeds the bed continues to show sliding friction behavior, but the porosity of the bed increases with increasing line speed.

7 NOMENCLATURE SLIDING FLOW REGIME.

C_D	Particle drag coefficient	-
C_{vt}	Delivered (transport) volumetric concentration	-
C_{vs}	Spatial volumetric concentration	-
d	Particle diameter	**m**
D_p	Pipe diameter	**m**
E_{rhg}	Relative excess hydraulic gradient	-
$E_{rhg,HeHo}$	Relative excess hydraulic gradient heterogeneous & homogeneous regimes	-
$E_{rhg,SF}$	Relative excess hydraulic gradient sliding flow regime	-
f	Particle diameter to pipe diameter ratio $f=d/(0.015 \cdot D_p)$	-
F_L	Durand & Condolios LDV Froude number	-
g	Gravitational constant 9.81 m/s^2	m/s^2
i_l	Hydraulic gradient pure liquid	**m/m**
i_m	Hydraulic gradient mixture	**m/m**
$i_{m,HeHo}$	Hydraulic gradient heterogeneous & homogeneous regimes	**m/m**
$i_{m,SB}$	Hydraulic gradient sliding bed regime	**m/m**
$i_{m,SF}$	Hydraulic gradient sliding flow regime	**m/m**
LDV	Limit Deposit Velocity	**m/s**
N	Zandi & Govatos parameter	-
R_{sd}	Relative submerged density	-
v_{ls}	Line speed	**m/s**
$v_{ls,ldv}$	Limit Deposit Velocity	**m/s**
μ_{sf}	Sliding friction factor	-

8 REFERENCES

Boothroyde, J., Jacobs, B. E., & Jenkins, P. (1979). Coarse particle hydraulic transport. *Hydrotransport 6: 6th International Conference on the Hydraulic Transport of Solids in Pipes.* (p. Paper E1). BHRA.

Doron, P., & Barnea, D. (1993). A three layer model for solid liquid flow in horizontal pipes. *International Journal of Multiphase Flow, Vol. 19, No.6.*, 1029-1043.

Durand, R., & Condolios, E. (1952). Etude experimentale du refoulement des materieaux en conduites en particulier des produits de dragage et des schlamms. (Experimental study of the discharge pipes materieaux especially products of dredging and slurries). *Deuxiemes Journees de l'Hydraulique.*, 27-55.

Gibert, R. (1960). Transport hydraulique et refoulement des mixtures en conduites. (Hydraulic transport and discharge pipes of mixtures). *Annales des Ponts et Chausees.*, 130(3), 307-74, 130(4), 437-94.

Gillies, R. G. (1993). *Pipeline flow of coarse particles, PhD Thesis.* Saskatoon: University of Saskatchewan.

Miedema, S. A. (June 2016). *Slurry Transport: Fundamentals, A Historical Overview & The Delft Head Loss & Limit Deposit Velocity Framework.* (1st Edition ed.). (R. C. Ramsdell, Ed.) Miami, Florida, USA: Delft University of Technology.

Ravelet, F., Bakir, F., Khelladi, S., & Rey, R. (2012). Experimental study of hydraulic transport of large particles in horizontal pipes. *Experimental Thermal and Fluid Science*, 13.

Sellgren, A., & Wilson, K. (2007). Validation of a four-component pipeline friction-loss model. *Hydrotransport 17* (pp. 193-204). BHR Group.

Vlasak, P., Chara, Z., Krupicka, J., & Konfrst, J. (2014). Experimental investigation of coarse particles water mixture flow in horizontal and inclined pipes. *Journal of Hydrology & Hydromechanics, Vol. 62(3).*, 241-247.

Vlasak, P., Kysela, B., & Chara, Z. (2012). FLOW STRUCTURE OF COARSE-GRAINED SLURRY IN A HORIZONTAL PIPE. *Journal of Hydrology & Hydromechanics, Vol. 60.*, 115-124.

Wiedenroth, W. (1967). *Untersuchungen uber die forderung von sand wasser gemischen durch rohrleitungen und kreiselpumpen.* Hannover: PhD Thesis, Technische Hochschule Hannover.

Wilson, K. C., Addie, G. R., & Clift, R. (1992). *Slurry Transport using Centrifugal Pumps.* New York: Elsevier Applied Sciences.

Yagi, T., Okude, T., Miyazaki, S., & Koreishi, A. (1972). *An Analysis of the Hydraulic Transport of Solids in Horizontal Pipes.* Nagase, Yokosuka, Japan.: Report of the Port & Harbour Research Institute, Vol. 11, No. 3.

Zandi, I., & Govatos, G. (1967). Heterogeneous flow of solids in pipelines. *Proc. ACSE, J. Hydraul. Div.,, 93(HY3).*, 145-159.